Large solid angle and high detection efficiency multi-element silicon drift detectors (SDD) for synchrotron based x-ray spectroscopy

Cite as: AIP Conference Proceedings **2054**, 060061 (2019); https://doi.org/10.1063/1.5084692
Published Online: 16 January 2019

J. Bufon, M. Altissimo, G. Aquilanti, P. Bellutti, G. Bertuccio, F. Billè, R. Borghes, G. Borghi, G. Cautero, S. Ciano, A. Cicuttin, D. Cirrincione, M. L. Crespo, S. Fabiani, F. Ficorella, M. Gandola, A. Gianoncelli, D. Giuressi, R. Grisonich, G. Kourousias, K. S. Mannatunga, F. Mele, R. H. Menk, L. Olivi, G. Orzan, A. Picciotto, A. Rachevski, I. Rashevskaya, M. Sammartini, S. Schillani, A. Stolfa, G. Zampa, N. Zampa, N. Zorzi, and A. Vacchi

Large Solid Angle and High Detection Efficiency Multi-element Silicon Drift Detectors (SDD) for Synchrotron Based X-ray Spectroscopy

J. Bufon[1,a)], M. Altissimo[1], G. Aquilanti[1], P. Bellutti[2,12], G. Bertuccio[3,4], F. Billè[1], R. Borghes[1], G. Borghi[2,12], G. Cautero[1,5], S. Ciano[5], A. Cicuttin[6,5], D. Cirrincione[7,5], M. L. Crespo[6,5], S. Fabiani[8,9], F. Ficorella[2,12], M. Gandola[3,4], A. Gianoncelli[1,5], D. Giuressi[1,5], R. Grisonich[1], G. Kourousias[1], K. S. Mannatunga[6,10], F. Mele[3,4], R. H. Menk[1,5,11], L. Olivi[1,5], G. Orzan[1], A. Picciotto[2,12], A. Rachevski[5], I. Rashevskaya[12], M. Sammartini[3,4], S. Schillani[1,5], A. Stolfa[1], G. Zampa[5], N. Zampa[5], N. Zorzi[2,12] and A. Vacchi[7,5]

[1]*Elettra Sincrotrone Trieste S.C.p.A., SS14 km 163.5, Trieste, Italy.*
[2]*Fondazione Bruno Kessler - FBK, Via Sommarive 18, Trento, Italy.*
[3]*Politecnico di Milano, Via Anzani 42, Como, Italy.*
[4]*INFN Milano, Via Celoria 16, Milano, Italy.*
[5]*INFN Trieste, Padriciano 99, Trieste, Italy.*
[6]*ICTP Mlab, Via Beirut 31, Trieste, Italy.*
[7]*University of Udine, Via delle Scienze 206, Udine, Italy.*
[8]*INAF IAPS, Via del Fosso del Cavaliere 100, Roma, Italy.*
[9]*INFN Roma Tor Vergata, Via della Ricerca Scientifica 1, Roma, Italy.*
[10]*University of Jayewardenepura, 21 Nawala Rd, Nugegada, Sri Lanka.*
[11]*University of Saskatchewan, 103 Hospital Drive, Saskatoon, Canada.*
[12]*TIFPA INFN, Via Sommarive 14, Trento. Italy.*

[a)]Corresponding author: jernej.bufon@elettra.eu

Abstract. Third and fourth generation light sources have revolutionized the research in many scientific and technological disciplines. New scientific challenges impose the construction of cutting-edge performance machines and experimental stations. In this context, off-the-shelf detection systems severely constrain the achievable results. These reasons motivated the ReDSoX research project, aiming to explore new solutions related to energy resolving imagers based on Silicon Drift Detectors (SDD), which are among the most employed acquisition devices in X-ray fluorescence spectroscopy. The main goal of the project is to develop novel versatile detection systems able to cover a large photoemission solid angle, being easily adaptable to the needs of different X-ray spectroscopy beamlines and ready to cope with high photon count-rates in order to exploit all the power of new light sources. Research efforts yielded two detector systems, dedicated to different experimental needs. The first system is composed of 32 SDD elements arranged on 4 monolithic sensors and covers a total non-collimated area of 1230 mm^2. Such device is optimized for detecting low-energy photons in the 200 – 4000 eV energy range. The second detector consists of a matrix of 64 SDD elements disposed on 8 monolithic arrays covering an overall non-collimated active area of 576 mm^2 and operating over an energy range between 4 and 30 keV. Both systems are highly integrated and can either be operated as an apparent large area single detector or as a multi-element detector, collecting information separately from each single element in order to enable spatially and angularly resolved advanced studies. The performances of the two detector systems have been studied at the TwinMic and XAFS beamlines (Elettra Sincrotrone Trieste, Italy), respectively. Recent results obtained during these measurements are presented and discussed.

Proceedings of the 13th International Conference on Synchrotron Radiation Instrumentation – SRI2018
AIP Conf. Proc. 2054, 060061-1–060061-7; https://doi.org/10.1063/1.5084692
Published by AIP Publishing. 978-0-7354-1782-3/$30.00

INTRODUCTION

With the widespread development of new generation synchrotron sources all over the world, the performance of detectors are in many cases no longer acceptable for novel experiments, even if they were state of the art only a few years ago, as they fail to exploit the potential of modern light sources. This also applies to Silicon Drift Detectors (SDD), which are among the most widely used devices in energy dispersive spectroscopy. SDDs have evolved considerably since the first prototype was produced and tested in 1984 [1] and the first large area detector was introduced [2]. Technological advancements contributed to a substantial decrease of the detectors leakage current and to design highly customized ultra low-noise front-end electronics, allowing the operation of large area detectors with good performances even at room temperature [3, 4]. In order to manage high count-rates without saturating the acquisition chain, it is necessary to distribute the charge collection among several electrodes (anodes) and processing channels, thus mitigating the pile-up and dead time phenomena. Since the leakage current is split between several anodes, and since different elements can be assembled in custom configurations, the production of large area multi-element detectors covering a wide solid angle is possible. This is indispensable and of paramount importance for applications where the events to be measured are rare.

The multi element approach made possible custom detector configurations according to the specific experimental requests, paying particular attention to the maximum expected count-rate and to the operation temperature, while maximizing the collection solid angle. Large-area, multi-element SDD systems made as singles monolithic device have indeed the advantage of minimizing dead space between detector elements. While such a configuration is advantageous for several aspects, it has, however, some drawbacks. Firstly, the large monolithic approach is not economically advantageous, since the production process yield is still limited. This makes likely for a large area multi-element detector to have elements with high leakage current, which would cause the entire detector to be discarded. In addition, a purely monolithic solution does not allow three-dimensional detector assemblies, e.g. surrounding the sample under examination with sensors in order to collect most of the emitted fluorescence photons. The two detection systems described here are a trade-off between a set of single-element detectors with large internal dead area and a single monolithic detector. Both are composed of 8-elements monolithic SDD arrays of different shapes, appropriately assembled to obtain the desired geometry.

Although the whole system consists of several independent detectors, it is highly integrated in terms of both back-end electronics, and acquisition software, which is unique for the entire instrument. This allows operating the device as a single, large area detector, thus providing a total aligned and calibrated spectrum, while maintaining the possibility to control every single element separately for advanced spatial and morphological studies [5].

TWO SETUPS FOR TWO DIFFERENT EXPERIMENTAL NEEDS

As mentioned above, it is fundamental to carefully design a custom detector to fully exploit the potential of new synchrotron light sources. In fact, there are no universal detectors suitable for all purposes. In this context, off-the-shelf detection systems severely constrain the achievable results. For this reason, the specific needs of two typical realities in which SDDs are mainly used were considered: soft X-ray spectroscopy, where high solid angle acquisition and energy resolution are of paramount importance, and X-ray absorption fine structure (XAFS) analysis, where the detectors have often to cope with very high count-rates. Taking into account the requirements on count-rate, energy resolution as well as the photon energies used at the TwinMic [6] and XAFS [7] beamlines of Elettra synchrotron (Italy) and XAFS beamline of the SESAME Middle Easts light source (Jordan), two detection systems based on multi-element SDDs were developed.

Low energy X-ray detection setup

In low energy X-ray fluorescence spectroscopy (LEXRF), the fluorescence yield is generally very low. Adding to this the low energy of the emitted photons, a vacuum environment and a large solid angle coverage are compulsory. Since organic materials are often subjects of study, a shallow detector entrance window is required to guarantee high efficiency even at very low photon energies, down to the carbon Kα emission line (277 eV). To provide large solid angle coverage, the multi-element approach allowed us to surround the sample with a pyramidal structure (Fig. 1b) consisting of four trapezoidal SDDs, each comprising eight square (6.2 x 6.2 mm^2) elements (Fig. 1a), for a total collimated area of 1113 mm^2 [8]. The collection solid angle results in 0.54π steradians or a coverage of about 27% of the hemisphere in which the sample emits XRF. The presented SDDs are specifically produced at FBK with a proprietary

technology featuring an ultrathin entrance window characterized by a thin dielectric layer covering a shallow uniform junction, assuring efficient collection of carriers generated close to the detector surface [9]. Furthermore, no other protective windows are interposed between the sample and the detector active surface in order to avoid any additional absorbing material.

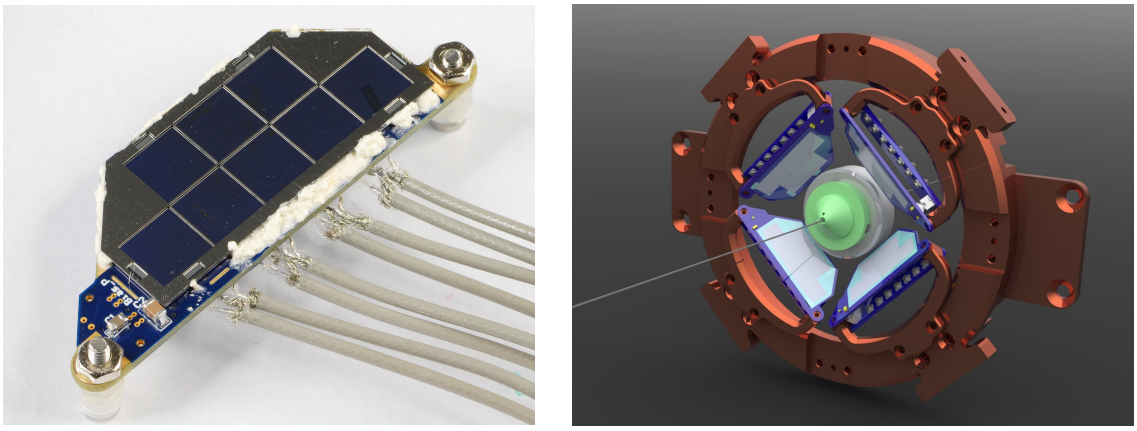

(a) (b)

FIGURE 1. The detection system designed for low energy X-ray fluorescence spectroscopy. Eight-element collimated SDDs (a) are arranged in a pyramidal geometry (b). The synchrotron beam impinges on the specimen placed a few millimeters downstream the central cone, generating X-ray fluorescence photons, which are then collected by the four detectors.

High count-rate XAFS setup

XAFS measurements are usually performed in transmission by means of ionization chambers. However, XRF acquisition mode becomes necessary when a specimen is highly diluted or highly absorbing in the energy range of the primary beam. Recently, there has been an increase in the number of experiments requiring XRF approach. Although the yield of specific fluorescence lines might be low, the overall photon flux attaining the detector is usually very high. Therefore, a single large area detector would suffer pile-up and saturation effects, which can be counter-balanced by increasing the distance of the detector from the analyzed sample, thus reducing the collection solid angle and consequently the data throughput. Multi-element detectors avoids this problem. The active area of the new XAFS SDD system is tiled up by 64 elements of 9 mm^2 each, assembled on 8 monolithic detectors [10] (Fig. 2), each equipped with a tungsten collimator, for a total collimated active area of 499 mm^2. The multi-element detectors assembly is accommodated in an aluminum housing in a controlled nitrogen atmosphere, isolated through a Mylar window, designed to be easily interfaced with different experimental environments.

Both XAFS and LEXRF sensors are fabricated on a 450-μm thick n-type silicon wafer with a resistivity of 9 kΩcm, which allows sufficient collection efficiency even for the most energetic photons encountered during XAFS measurements.

Signal conditioning and data acquisition chain

The front-end and the whole acquisition chain follow the same pattern for both setups, except for slight differences according to the specifications of the two particular cases. The first read-out stage is entrusted to the ultra-low noise SIRIO charge sensitive preamplifier [11], specifically designed in two versions for the two different applications. The preamplifier output signals, one for each detector element, are filtered and further amplified by CR-RC^2 analogue pre-shaper with a selectable shaping time. The peak-shaped signals are sampled by multichannel ADCs with a resolution of 12 bits at 40 MHz sampling rate and further filtered with trapezoidal finite impulse response (FIR) filters of variable length and adaptive coefficients in order to guarantee the maximum energy resolution in each environment [12]. Digital filtering, settings and complete monitoring of the instrument are made by high performance FPGAs, which send the acquired data to a host computer via TCP/IP protocol. Both developed instruments respond to a series of 8-bit basic commands, easy to implement in any beamline control software. Moreover, a dedicated high-level software has been

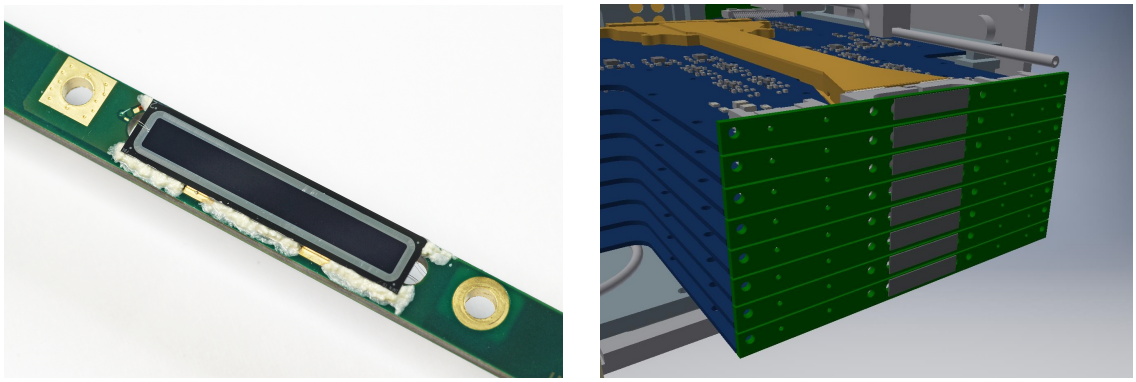

(a) (b)

FIGURE 2. The XAFS fluorescence detector system based on monolithic arrays of eight SDDs (a), assembled as a matrix of 64 elements (b).

developed for an easy and immediate way to operate the new multi-element detector systems, also offering some useful X-ray fluorescence measurements utilities.

EXPERIMENTAL RESULTS AND DETECTORS PERFORMANCES

The best way to verify detectors proper functionality is to test it in the final working environments. In this case, the two detection systems were tested on the TwinMic and XAFS beamlines respectively. In order to be well prepared for the synchrotron beam test, the new detection systems have been extensively characterized with traditional radiation sources as well.

The energy resolution of SDDs has been measured on the Mn Kα emission line, which can be obtained with a ^{55}Fe radioactive source or by a Mn target exposed to a photon or electron beam. The 8-element trapezoidal SDDs show an average energy resolution below 130 eV full width at half maximum (FWHM) at 5.9 keV at a temperature of -20 °C. This energy resolution was obtained with a trapezoidal FIR filter with a peaking time of 4 μs and a flat top of 100 ns. On the other side, the minute dimensions of the XAFS detection system elements (77% smaller than the LEXRF system SDDs) and an average leakage current below 100 pA/cm^2 at +20 °C on both detectors, allow satisfactory performances even at room temperature. Tests on XAFS SDD arrays show a typical energy resolution of around 165 eV FWHM at +25 °C and below 150 eV FWHM with moderate cooling (+10 °C measured on the detector on-board thermistors) using a 1.6 μs peaking time with a flat top of 50 ns.

For energies below 2 keV, which is the operating range of the TwinMic beamline, the energy resolution on the Mn Kα line is no longer a sufficient parameter to characterize a detector. The energy resolution is therefore also quoted for lower emission lines, typically fluorine Kα (677 eV), where the multi-element LEXRF detection system show a FWHM of 83 eV at -10 °C.

The energy resolution at low energies is strongly affected not only by noise, but also by incomplete charge collection. A peak to background measure was made with a ^{55}Fe X-ray source for a general indication of the charge collection efficiency. Comparing the height of the Mn Kα peak to the average background between 0.9 and 1.1 keV a ratio of about 11000:1 was obtained. However, this measure does not ensure good peak shapes for low energy X-rays, which only penetrate a short distance into the semiconductor. In fact, low-energy X-rays are absorbed in the very interfacial layers of the entrance window, where the generated carriers might be partially or completely lost in the dielectric layer and at the dielectric-silicon interface, or cannot be efficiently separated by the low electric field at the interface side of the junction. The corresponding charge loss leads to deterioration of both the efficiency and the energy resolution.

In order to gain information about the sensitivity to incomplete charge collection at low energies, the energy resolution at carbon Kα line (277 eV) has been measured (Fig. 3). A value of 75 eV FWHM at -10 °C on C Kα together with 83 eV on F Kα indicates that the system noise contribution is about 70 eV, considerably worse than what was measured on the Mn Kα line, where the system noise contribution was estimated around 50 eV. The reason of this discrepancy is related to incomplete charge collection and the disturbance of the photoemitted electrons reaching

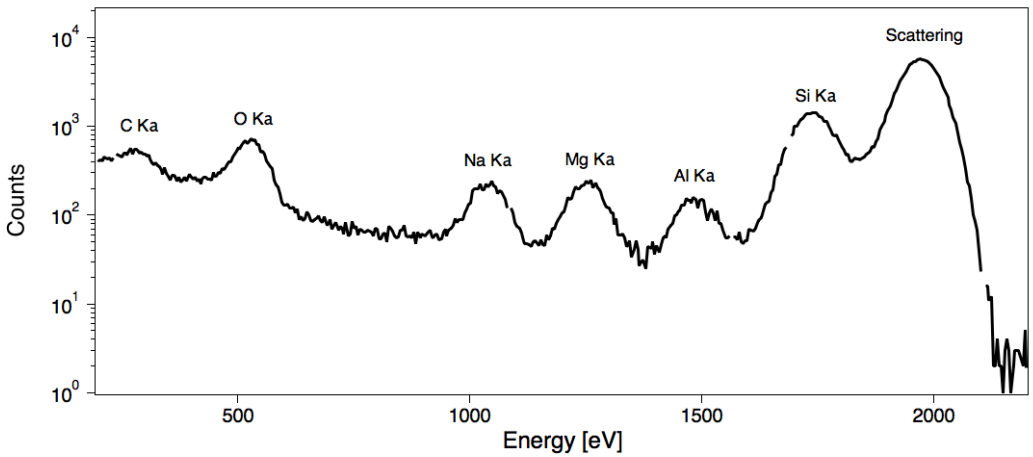

FIGURE 3. X-ray fluorescence spectrum of a biological sample acquired on the TwinMic beamline of Elettra Sincrotrone Trieste. The figure show C (277 eV), O (525 eV), Na (1041 eV), Mg (1254 eV), Al (1487 eV) and Si (1740 eV) Kα emission lines and the synchrotron photon beam elastic peak (near 2 keV).

the detector in vacuum. To ensure that X-rays, but no electrons, enter the detector, a deposition of a few nanometers of aluminum and titanium on the entrance window is planned. This should discharge the incoming electrons on the detector guards with negligible effects on photon absorption. The issue of incomplete charge collection will be investigated and the possibility of a further improvement of the entrance window performances, by a proper optimization of the technological parameters, will be evaluated.

Besides energy resolution, another challenge in light element detection is indeed the detector efficiency. Owing to the windowless concept and a very thin detector entrance window the detection efficiency at the C Kα line is at least 60% (based on Geant4 [13] Monte Carlo simulations).

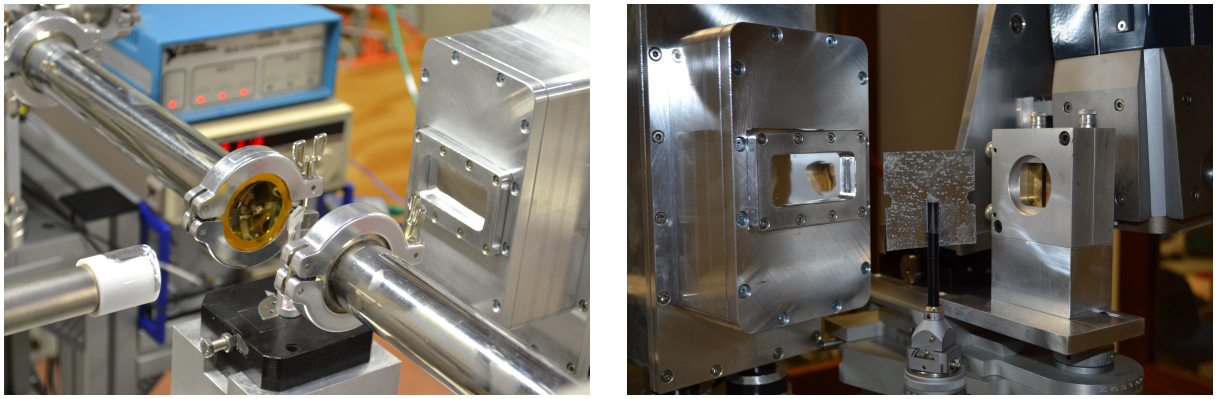

(a) (b)

FIGURE 4. Count-rate tests on the XAFS detection system at the XAFS beamline (a) and with a multi-anode X-ray tube in the hard and soft X-ray optical engineering laboratory (b).

A prototype of the XAFS fluorescence detection system, consisting of two 8-element modules, mounted in the central positions of the detector housing, was tested at the XAFS beamline and in the Hard & Soft X-ray Optical Engineering Laboratory, both at Elettra Sincrotrone Trieste (Fig. 4). The main goal of the tests was to confirm the ability of the new system to work at high input count-rates (ICR) while maintaining low dead time and a good energy resolution. Experimental results confirmed the targeted design parameters, reaching a maximum acquisition rate of 3.1 Mcounts/cm^{2}s with a peaking time of 0.4 μs (Fig. 5). This translates into an output count-rate (OCR) of 15.5 Mcount/s for the entire 64 elements collimated detector.

There is obviously a trade-off between energy resolution and short signal process time (which permits high throughputs). The maximum OCR was obtained with a peaking time of 0.4 μs; the energy resolution was around 175 eV FWHM at Mn Kα. The longer is the shaping time, the lower is the white voltage noise. Being the leakage current for a single XAFS 9 mm^2 SDD element as low as 10 pA at 20 °C, the energy resolution is improved by increasing the shaping time towards some microseconds. As mentioned above, an energy resolution below 150 eV FWHM at Mn Kα line was measured using 1.6 μs peaking time. With this peaking time the maximum achievable OCR results around 1 Mcounts/cm^{2}s, however with a slightly worse energy resolution (155 eV FWHM at Mn Kα) a maximum OCR of 1.6 Mcounts/cm^{2}s was obtained with 0.9 μs peaking time.

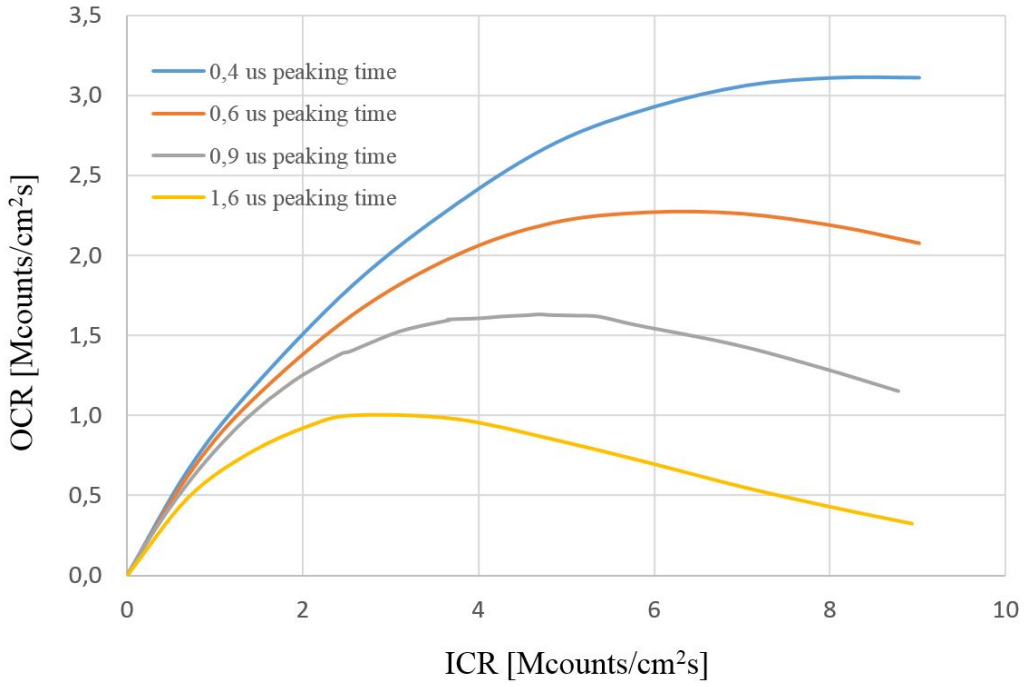

FIGURE 5. Output count-rate (OCR) versus input count-rate (ICR), obtained with different peaking time ranging from 0.4 to 1.6 μs.

CONCLUSIONS AND PERSPECTIVES

To fully exploit the potential of beamlines, a detection system should ideally detect all the emitted photons. This leads to a large solid angle detector able to handle high count-rates without saturating the acquisition chain. The two systems presented here try to satisfy these needs. The detector designed for LEXRF spectroscopy covers a solid angle equal to 27% of the XRF emission hemisphere. This allows a considerable reduction in duration of measurements, which would be at least of an order of magnitude longer when performed with standard SDDs. XAFS measurements, on the other hand, requires the ability of measuring large photon flows without saturating the detector. For this purpose a highly pixelated detector divided into 64 small elements has been designed, fabricated and tested. Thanks to its multi-element structure and a fast acquisition and processing electronics, it is possible to manage high count-rates up to a maximum of about 15 Mcounts/s on the entire detection system.

Both systems were tested on the target beamlines yielding good results and achieving the main design goals. During the tests, however, some problems emerged, which will be addressed by the next prototypes. A solution to improve the incomplete collection at low photon energies will be investigated together with a shield to avoid the disturbance of photoemitted electrons hitting the sensor. For the XAFS detection system an improved cooling has been designed that would allow the detector to operate at 0 °C, thereby improving the energy resolution. Moreover, a new version of SIRIO preamplifier is under design to further lower the system noise. A new, more versatile housing

is being studied, which will allow to attach the XAFS detection system directly to experimental chambers operating in vacuum.

Multi-element detection systems open new perspectives for X-ray research, allowing an increasing number of possible experiments by reducing the acquisition time, thanks to the large solid angle coverage. Additional advantages are granted by the multi-element approach, such as spatial information. Owing to the acquisition based on FPGAs operating at high clock frequencies, information of the arrival time of each detected photon could also be exploited, allowing time-resolved acquisitions.

ACKNOWLEDGMENTS

This work has been carried out within the ReDSoX-2 INFN research project, supported with the contribution of the Italian Ministry of University and Research within the EUROFEL Project and the contribution of Fondazione Bruno Kessler (FBK). We thank all the staff of the Hard & Soft X-ray Optical Engineering Laboratory and TwinMic and XAFS beamlines of Elettra for the support during the test measurements.

REFERENCES

[1] E. Gatti, P. Rehak, and J. T. Walton, *Nucl. Instrum. Meth. A*, **226**, 129–141 (1984).

[2] A. Vacchi, P. Cox, A. Giacomelli, P. Castoldi, S. Chinnici, E. Gatti, A. Longoni, F. Palma, M. Sampietro, P. Rehak, G. Ballocchi, J. Kemmer, and P. Holl, *Nucl. Instrum. Meth. A*, **326**, 267–272 (1993).

[3] G. Bertuccio, M. Ahangarianabhari, C. Graziani, D. Macera, Y. Shi, A. Rachevski, I. Rashevskaya, A. Vacchi, G. Zampa, N. Zampa, P. Bellutti, G. Giacomini, A. Picciotto, and C. Piemonte, *J. Instrum.*, **10**, p. P01002 (2015).

[4] G. Bertuccio, D. Macera, C. Graziani, and M. Ahangarianabhari, *IEEE T. Nucl. Sci.*, **63**, 400–406 (2016).

[5] F. Billè, G. Kourousias, E. Luchinat, M. Kiskinova, and A. Gianoncelli, *Spectrochim. Acta B*, **122**, 23–30 (2016).

[6] A. Gianoncelli, G. Kourousias, L. Merolle, M. Altissimo, and A. Bianco, *J. Synchrotron Radiat.*, **23**, 1526–1537 (2016).

[7] A. Cicco, G. Aquilanti, M. Minicucci, E. Principi, N. Novello, A. Cognigni, and L. Olivi, *J. Phys. Conf. Ser.*, **190**, p. 012043 (2009).

[8] J. Bufon, S. Schillani, M. Altissimo, P. Bellutti, G. Bertuccio, F. Billè, R. Borghes, G. Borghi, G. Cautero, D. Cirrincione, S. Fabiani, F. Ficorella, M. Gandola, A. Gianoncelli, D. Giuressi, G. Kourousias, F. Mele, R. H. Menk, A. Picciotto, A. Rachevski, I. Rashevskaya, M. Sammartini, A. Stolfa, G. Zampa, N. Zampa, N. Zorzi, and A. Vacchi, *J. Instrum.*, **13**, p. C03032 (2018).

[9] W. Chen, G. Carini, J. Keister, Z. Li, and P. Rehak, *IEEE T. Nucl. Sci.*, **54**, 1842 – 184810 (2007).

[10] S. Fabiani, M. Ahangarianabhari, G. Baldazzi, P. Bellutti, G. Bertuccio, M. Bruschi, J. Bufon, S. Carrato, A. Castoldi, G. Cautero, S. Ciano, A. Cicuttin, M. Crespo, M. Dos Santos, M. Gandola, G. Giacomini, D. Giuressi, C. Guazzoni, R. H. Menk, J. Niemela, L. Olivi, A. Picciotto, C. Piemonte, I. Rashevskaya, A. Rachevski, L. P. Rignanese, A. Sbrizzi, S. Schillani, A. Vacchi, V. Villaverde Garcia, G. Zampa, N. Zampa, and N. Zorzi, *J. Phys. Conf. Ser.*, **689**, p. 012017 (2016).

[11] G. Bertuccio, D. Macera, C. Graziani, and M. Ahangarianabhari, "A cmos charge sensitive amplifier with sub-electron equivalent noise charge," (Seattle, USA, 2014), pp. 8–15.

[12] V. T. Jordanov and G. F. Knoll, *Nucl. Instrum. Meth. A*, **345**, 337–34506 (1994).

[13] J. Allison, K. Amako, J. Apostolakis, P. Arce, M. Asai, T. Aso, E. Bagli, A. Bagulya, S. Banerjee, G. Barrand, B. Beck, A. Bogdanov, D. Brandt, J. Brown, H. Burkhardt, P. Canal, D. Ott, S. Chauvie, K. Cho, H. Yoshida, and et al., *Nucl. Instrum. Meth. A*, **835**, 186–225 (2016).